https://doi.org/10.1093/plphys/kiad248 PLANT PHYSIOLOGY 2023: 192: 2687–2702

Plant Physiology®

Research Article

WAVE-DAMPENED2-LIKE4 modulates the hyper-elongation of light-grown hypocotyl cells

Kristina Schaefer,[1] Ariadna Cairo Baza,[1] Tina Huang,[1] Timothy Cioffi,[1] Andrew Elliott[1] and Sidney L. Shaw[1,*]

1 Department of Biology, Indiana University, Bloomington, IN 47405, USA

*Author for correspondence: sishaw@indiana.edu
The author responsible for distribution of materials integral to the findings presented in this article in accordance with the policy described in the Instructions for Authors (https://academic.oup.com/plphys/pages/general-instructions) is: Sidney L. Shaw (sishaw@indiana.edu).

Abstract

Light, temperature, water, and nutrient availability influence how plants grow to maximize access to resources. Axial growth, the linear extension of tissues by coordinated axial cell expansion, plays a central role in these adaptive morphological responses. Using Arabidopsis (*Arabidopsis thaliana*) hypocotyl cells to explore axial growth control mechanisms, we investigated *WAVE-DAMPENED2-LIKE4* (*WDL4*), an auxin-induced, microtubule-associated protein and member of the larger *WDL* gene family shown to modulate hypocotyl growth under changing environmental conditions. Loss-of-function *wdl4* seedlings exhibited a hyper-elongation phenotype under light conditions, continuing to elongate when wild-type Col-0 hypocotyls arrested and reaching 150% to 200% of wild-type length before shoot emergence. *wdl4* seedling hypocotyls showed dramatic hyper-elongation (500%) in response to temperature elevation, indicating an important role in morphological adaptation to environmental cues. *WDL4* was associated with microtubules under both light and dark growth conditions, and no evidence was found for altered microtubule array patterning in loss-of-function *wdl4* mutants under various conditions. Examination of hormone responses showed altered sensitivity to ethylene and evidence for changes in the spatial distribution of an auxin-dependent transcriptional reporter. Our data provide evidence that *WDL4* regulates hypocotyl cell elongation without substantial changes to microtubule array patterning, suggesting an unconventional role in axial growth control.

Introduction

Flowering plants are sessile organisms that alter their morphology in response to environmental changes. Light, temperature, moisture, and nutrients are detected through an array of sensory mechanisms that lead to systemic changes in phytohormone levels (Verma et al. 2016). Phytohormones coordinate plant growth at the cell and tissue levels, leading to repositioning of plant organs and modulation of plant surface area in accordance with the perceived stimuli. These larger adaptive mechanisms allow plants to optimize nutrient uptake even under extreme conditions (Reid and Hayes 2003, Elbasiouny et al. 2022).

Stems and roots undergo axial growth, coordinating 1D extension of constituent cells to produce tissue elongation and tropic responses. Axial cell growth is special in that it requires extension of the lateral cell walls (i.e. along the growth axis) without extension of the apical and basal anticlinal cell walls. To affect that process, plants create highly anisotropic cell wall materials in the lateral walls that extend preferentially along the plant axis (Cosgrove 2005). The material anisotropy arises when microtubules at the cell cortex form coaligned patterns transverse to the plant growth axis (Elliott and Shaw 2018), acting as guides for the cellulose deposition (Paredez et al. 2006, Oda 2015). When the wall is acidified to trigger changes in bonding, the long cellulose polymers radially reinforce the wall, leading to preferential axial extension under turgor (Cosgrove 2005). This mechanism, in large part, allows for the coordinated extension of connected cells with immediately adjoining walls.

Received December 08, 2022. Accepted March 21, 2023. Advance access publication April 25, 2023

Hypocotyl cells in the Arabidopsis (*Arabidopsis thaliana*) seedling serve as an important model for investigating axial growth mechanisms rarely undergoing cell division and remaining extremely sensitive to environmental cues (Gendreau et al. 1997, Vandenbussche et al. 2005, Braidwood et al. 2014). The phytohormones, auxin, brassinosteroid (BR), and ethylene, modulate apical hook opening, tropic bending, and hyper-elongation of the hypocotyl in response to environmental stimuli such as light and temperature (Esmon et al. 2005, Vandenbussche et al. 2005, Verma et al. 2016). Exogenous application of these hormones causes hyper-elongation of light-grown hypocotyls, where auxin and BRs have determinant effects on cortical microtubule array patterning (Shibaoka 1994, Vineyard et al. 2013, Elliott and Shaw 2018, True and Shaw 2020).

WAVE-DAMPENED2-LIKE4 (*WDL4*) is a conserved member of the WDL gene family, having homology to animal *targeting protein for Xklp2* (TPX2) genes that serve as microtubule nucleation factors on condensed chromatin (Smertenko et al. 2021). The WDL3 and WDL5 family members bind microtubules and effect hypocotyl elongation in response to various environmental conditions. WDL3 inhibits hypocotyl elongation after light exposure and is degraded by CONSTITUITIVE PHOTOMORPHOGENIC 1 (COP1) in the dark (Liu et al. 2013, Lian et al. 2017). WDL5, in contrast, inhibits hypocotyl elongation in dark-grown seedlings and in response to ethylene (Sun et al. 2015). In both cases, the hypocotyl elongation phenotype was attributed to an inability of the mutants to correctly pattern cortical microtubules (Liu et al. 2013, Sun et al. 2015). WDL4 is transcriptionally regulated by ethylene and shown to play a role in apical hook opening in etiolated hypocotyls (Deng et al. 2021). Unlike WDL3 and WDL5, WDL4 did not exhibit a specific effect on cortical microtubule arrays in the apical hook, despite evidence of microtubule association (Deng et al. 2021). A possible link to auxin signaling was inferred for WDL4 through connections to the secretory pathway and auxin transporter proteins (Deng et al. 2021).

In this work, we examined the specific role of WDL4 in directing the axial growth of hypocotyl cells. Our prior work indicates that auxin plays a key role in coordinating cortical microtubule array patterning with axial cell growth in the hypocotyl (Vineyard et al. 2013, Elliott and Shaw 2018, True and Shaw 2020). WDL4 was strongly upregulated in the hypocotyl by exogenous auxin (Chapman et al. 2012) and previously shown to associate with cortical microtubules and function in the unhooking of the etiolated hypocotyl without an effect on the microtubules (Deng et al. 2021). We, therefore, asked if WDL4 could be further acting to regulate axial cell growth more generally during hypocotyl maturation and in response to environmental cues.

Results

WDL4 inhibits hypocotyl extension in light-grown seedlings

To investigate the effects of *WDL4* on axial growth, we compared hypocotyl lengths for wild type (Col-0), a *WDL4* tDNA insertion mutant in Col-0 (*wdl4*) (Supplemental Fig. S1A), and Col-0 seedlings constitutively expressing full-length genomic *WDL4* fused to the monomeric yellow-green fluorescent protein (mNEON) (Shaner et al. 2013) (35s:WDL4-mNeon) (Fig. 1, A to I). Seedlings were grown at 22 °C under a 12/12 h light/dark cycle and measured from 3 to 6 days post germination (dpg). Wild-type hypocotyls reached an average length of 0.67 ± 0.14 mm by 3 dpg and extended to 0.76 ± 0.18 mm by 4 dpg ($n > 55$ for all measures) (Fig. 1A and J). By 5 dpg, hypocotyl elongation arrested at 0.81 ± 0.18 mm, measuring 0.79 ± 0.20 mm at 6 dpg, with first leaves visible by 7 dpg (Fig. 1A and J). In comparison, *wdl4* hypocotyls were significantly longer, extending to 0.81 ± 0.14 mm at 3 dpg and 1.08 ± 0.21 mm by 4 dpg ($P < 0.0001$, 2-tailed t-test for all P values except where noted) or 120% and 140% of wild type, respectively (Fig. 1B and K). Importantly, *wdl4* hypocotyls continued to grow, reaching 1.59 ± 0.37 mm by 5 dpg and to 2.07 ± 0.43 mm by 6 dpg (195% and 250% of wild-type length, respectively), indicating a hyper-elongation phenotype due primarily to continued growth beyond 4 dpg (Fig. 1B and K). Constitutive WDL4 expression had no significant effect on hypocotyl length at 3 to 6 dpg when compared to wild-type plants ($P > 0.05$, $n > 49$) (Fig. 1C, J, and L). Leaf emergence occurred between 6 and 7 dpg in *wdl4* and constitutive WDL4 plants (Fig. 1, A to C), indicating no substantial delay of meristem development.

To determine if the hyper-elongation phenotype was exacerbated by light/dark transitioning (Vandenbussche et al. 2005), we measured hypocotyl length under continuous (24 h) light at 22 °C. Wild-type hypocotyls were 10% to 20% longer under continuous light compared to light-cycled, but hypocotyls still arrested by 5 dpg (Fig. 1D and M). The *wdl4* hypocotyls in continuous light were slightly longer than *wdl4* under light-cycled conditions (Fig. 1E and N). The *wdl4* hypocotyls reached 140% of wild type by 3 dpg, 160% by 4 dpg, 220% by 5 dpg, and 277% at 6 dpg indicating the same hyper-elongation phenotype under continuous light driven by the absence of growth arrest at 5 dpg (Fig. 1M and N). Constitutive *WDL4* expression (Fig. 1F) resulted in a mild (~10%) but significant ($n > 25$, $P < 0.05$) reduction in hypocotyl length for continuous light at days 3 to 5 postgermination, but ultimately showed no significant effect ($P > 0.05$, $n > 35$) by 6 dpg, compared to wild-type seedlings (Fig. 1M and O).

Seedlings grown in continuous darkness produced substantially longer, etiolated hypocotyls in all backgrounds (Fig. 1, G to I). Dark-grown *wdl4* seedlings showed no significant difference in hypocotyl lengths compared to wild type ($P>>0.05$, $n > 46$) at 3 to 6 dpg (Fig. 1P and Q). Constitutive WDL4 expression, however, resulted in a significant reduction in hypocotyl length ($P<<0.05$, $n > 45$) for 3 to 6 dpg when compared to wild type, reaching 82%, 65%, 64%, and 62% of wild type, respectively (Fig. 1P and R). Together, these data indicated that *WDL4* plays a role in retarding axial hypocotyl elongation, specifically in light-grown seedlings, with most of the hyper-elongation occurring after wild-type hypocotyls arrest growth.

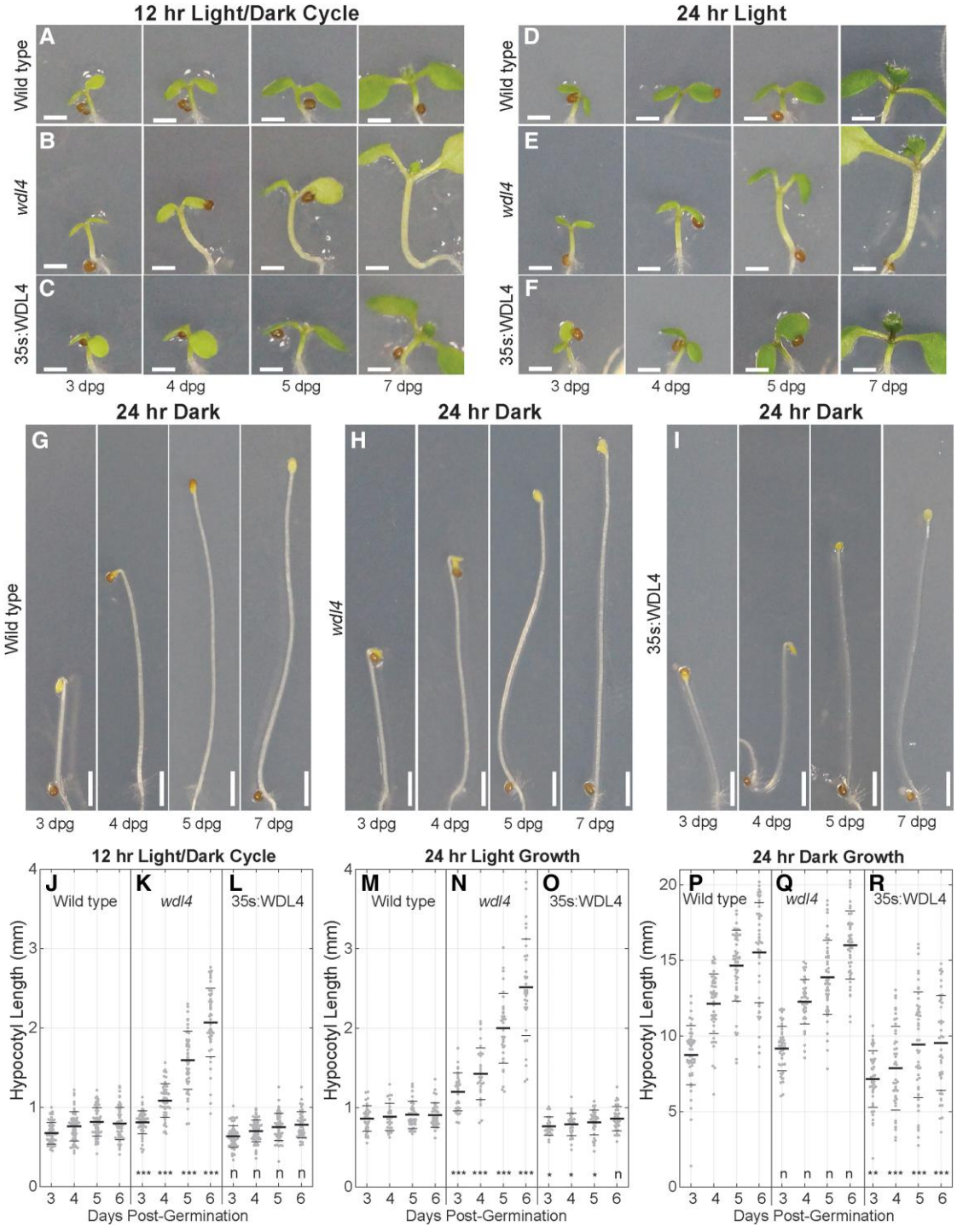

Figure 1. WDL4 inhibits axial hypocotyl extension in light-grown seedlings. Representative images of *Arabidopsis* seedling growth for **A)** wild type, **B)** *wdl4*, and **C)** wild type ectopically expressing WDL4 (35s:WDL4) from 3 to 6 d postgermination at 22 °C under a 12/12 h light/dark cycle and replicated under both continuous (24 h) light **D to F)** and continuous (24 h) dark **G to I)**. Leaf emergence was observed by day 7 for all backgrounds under lighted conditions. Hypocotyl length measured from light-cycled seedlings showing **J)** wild type extending from days 3 to 5 before growth arrest, **K)** *wdl4* hyper-extension through day 6, and **L)** 35:WDL4 lines equivalent to wild type. Wild-type seedlings grown under continuous (24 h) light **M)** had slightly longer hypocotyls than light cycled plants but still arrested axial growth by day 5. Continuous light significantly increased *wdl4* hypocotyl length **N)** compared to light-cycled *wdl4* plants where 35s:WDL4 expression **O)** had no significant effect. Comparison of dark-grown wild-type **P)** and *wdl4* **Q)** seedlings showed no difference in hypocotyl length between days 3 and 6. Ectopic 35s:WDL4 **R)** significantly reduced hypocotyl length in continuous darkness compared to wild type. Dots represent individual seedlings, thick bar is mean value, and thin bars are standard deviation. All *P*-values are derived from 2-tailed t-test comparing the same age wild type. $^{*}P < 0.05$, $^{**}P < 0.001$, $^{***}P < 0.0001$, *n* = nonsignificant. Scale bar = 1 mm for images **A to F)**, scale bar = 2 mm for **G to I)**.

To verify that that the *wdl4* growth phenotype was due to a loss of *WDL4* function, we expressed a full-length genomic WDL4 transgene fused to an mNeon fluorescent protein under the native promoter (pWDL4:WDL4-mNeon) in the *wdl4* mutant background. Hypocotyl lengths were measured for wild type, *wdl4*, and pWDL4:WDL4-mNeon lines at 3 to 5 dpg under 24 h lighted conditions (Supplemental Fig. S1B). At 3 dpg, pWDL4:WDL4-mNeon hypocotyls were slightly longer than wild type ($P < 0.05$, $n > 32$ seedlings), but by 4 and 5 d, pWDL4:WDL4-mNeon seeding lengths were indistinguishable from wild type ($P = 0.8819$, 0.2664, respectively).

WDL4 specifically regulates cell elongation

Mutations in tubulin or microtubule-associated proteins altering the cortical microtubule array patterning typically produce cells with more isotropic shapes or alterations in tissue extension producing twists or skewing. To examine cell morphology, we imaged 4 dpg propidium iodide-stained seedlings grown in constant light using laser scanning confocal microscopy (LSCM) (Fig. 2, A to D). The number of cells per hypocotyl cell file for wild type (19.5 ± 2.3 cells/file, $n = 4$ plants, 234 cells) and *wdl4* (20.2 ± 2.9 cells/file, $n = 4$ plants, 202 cells) confirmed that the hyper-elongation phenotype was driven by cell elongation and not by cell proliferation. Comparison of wild-type and *wdl4* cells indicated that the mutant had elongated cells with no obvious swelling, gross changes in cell shape, or deviations in cross-wall orientation (Fig. 2, C and D). Plotting cell length against cell width for individual *wdl4* cells indicated a specific difference in cell elongation without a proportional change in radial cell expansion (Fig. 2E). Comparing cell lengths and widths as a function of normalized hypocotyl length (Fig. 2, F and G), *wdl4* showed an increase in mean cell length beginning near the base, peaking just before the hypocotyl midpoint, and tapering to shorter lengths toward the apex, similar to cell length profiles for dark-grown hypocotyls (Gendreau et al. 1997). Average cell width in *wdl4* plants was nearly constant and not statistically distinguishable from wild-type average cell width plotted over the normalized hypocotyl length (Fig. 2, F and G). Together, these data provide evidence that the absence of *WDL4* function leads to a hyper-elongation of the hypocotyl cells with no evidence for disproportionate cell swelling, twisting, or proliferation.

WDL4 associates with all cortical microtubules in hypocotyl cells

LSCM images of 5 dpg pWDL4:WDL4-mNeon hypocotyls showed that WDL4 appeared in all epidermal hypocotyl cells under both light-grown and dark-grown conditions (Fig. 3, A and B) with no obvious increase or redistribution between 3 and 4 dpg when hypocotyl elongation normally arrests (Supplemental Fig. S2). To investigate the extent of WDL4 cortical microtubule association, we crossed pWDL4:WDL4-mNeon to a Col-0 line constitutively expressing a genomic *BETA-TUBULIN 1* (TUB1) gene having an N-terminally fused mSCARLET fluorescent protein (RFP-TUB1). WDL4-mNeon colocalized with microtubules throughout the cell cortex (Fig. 3, C to F). Colocalization was observed on all cell faces to the extent that the signal to noise for the natively expressed WDL4 allowed for observation (Fig. 3, C to F). The dependence of WDL4 localization on microtubules was verified by concurrent loss of localizations for WDL4-mNeon and RFP-TUB1 in plants treated with the microtubule depolymerizing agent, oryzalin (15 μM), and imaged at 8 and 51 min posttreatment (Fig. 3, G and H).

To examine WDL4 localization in transverse microtubule array patterns, we induced pWDL4:WDL4-mNeon seedlings to reorganize the cortical arrays with an exogenous light-stable synthetic auxin, picloram (5 μM) (Hamaker et al. 1963). We observed continuous colocalization of WDL4-mNeon with RFP-TUB1 labeled cortical microtubules in transverse patterns at 2 h postinduction (Fig. 3, I and J).

Cortical microtubule array patterning is not affected by loss of WDL4 function

Axial cell growth depends upon the correct patterning of cellulose microfibrils into cell walls templated by transverse cortical microtubule arrays (Oda 2015). To determine if the microtubule arrays in *wdl4* showed substantial changes in microtubule number or basal dynamics, we crossed the *wdl4* mutant into a Col-0 *END BINDING 1* (35s:GFP-EB1b) reporter line that labels growing microtubule plus-ends (Mathur et al. 2003). Ten-frame time-lapse observations taken at 3 s intervals using LSCM (Elliott and Shaw 2018) indicated that the average density of growing microtubule plus ends for wild type (0.28/μm^2, $n = 4{,}139$ trajectories from 15 cells) and *wdl4* (0.26/μm^2, $n = 18{,}274$ trajectories from 22 cells) was statistically indistinguishable ($P >> 0.05$, 2-tailed t-test). Additionally, GFP-EB1b velocities, indicating microtubule polymerization rate, in wild type (6.27 ± 1.70 μm/min) and *wdl4* (6.27 ± 1.71) were not significantly different ($P = 0.99$; 2-tailed t-test).

Loss of *WDL4* function resulted in a continuation of axial hypocotyl growth after 4 dpg in continuous lighted conditions (Fig. 1). We, therefore, hypothesized that light-grown *wdl4* would exhibit a higher percentage of transverse array patterns at 5 dpg when compared to wild type (Shibaoka 1994, Sedbrook and Kaloriti 2008, Vineyard et al. 2013, Oda 2015). To test this hypothesis, we imaged live seedlings expressing a GFP-TUB1 transgene in the wild type, *wdl4*, or constitutive 35s:WDL4 expression background (Fig. 4, A to C). Microtubule array patterns were designated as longitudinal, oblique, transverse, or basket as previously described (Granger and Cyr 2001, Vineyard et al. 2013). The percentage of cells in each array pattern class indicated no critical difference in microtubule array pattern distribution between wild type and *wdl4* and a modest decrease in transverse patterns for the constitutively expressed 35s:WDL4 lines ($P < 0.03$, 2-sided rank sum test of normalized counts) (Fig. 4G). Experiments comparing array pattern distribution between

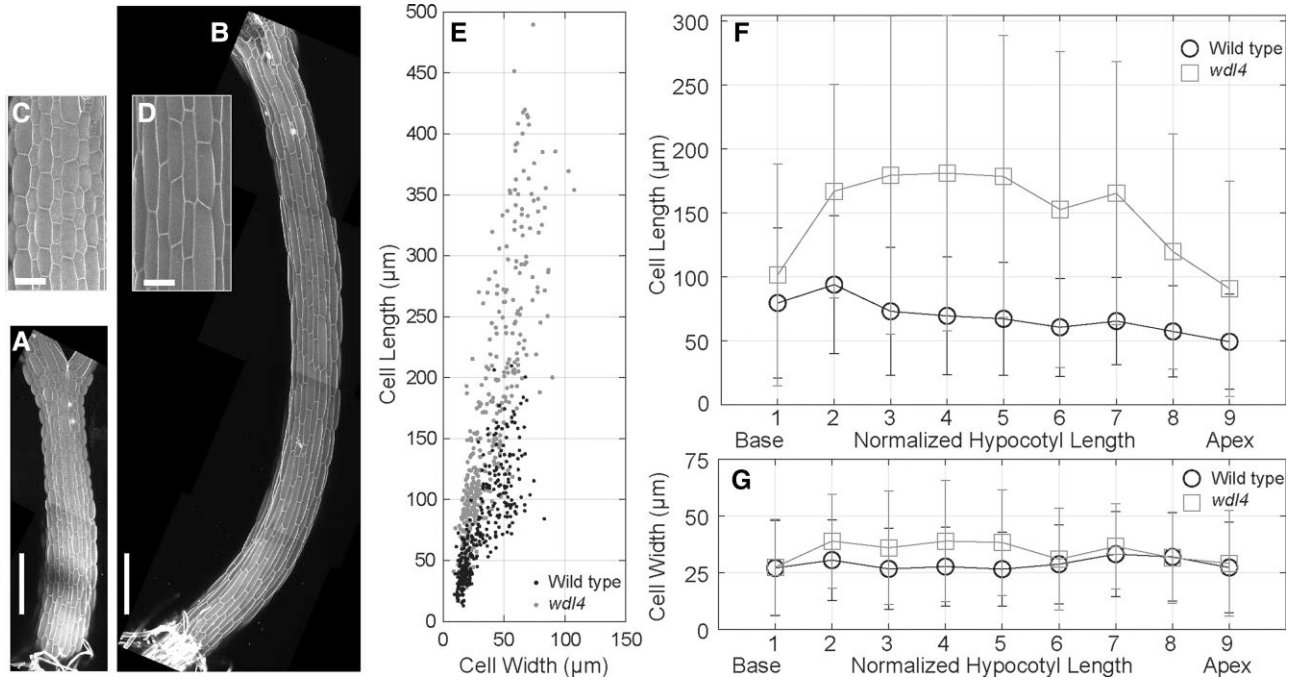

Figure 2. The *wdl4* mutant increases cell length without proportional change to cell width. Composite confocal microscopy projections of propidium iodide-stained hypocotyls from wild type **A)** and *wdl4* **B)** at 4 dpg grown under continuous light. Scale bar = 250 μm. Insets of wild type **C)** and *wdl4* **D)** indicating no gross cell morphology changes. Scale bar = 50 μm. **E)** Scatter plot of cell width and cell length taken from 2 adjacent cell files from 5 wild type (red) and 5 *wdl4* (cyan) seedlings at 4 dpg grown in constant light indicating axial cell extension in *wdl4*. Averaged cell lengths **F)** and widths **G)** with standard deviations from base to apex of the normalized hypocotyl length. Wild-type cells (○) are longest at the base of hypocotyl and *wdl4* (□) cells are longest in the middle of the hypocotyl with approximately equal average cell width.

wild type and *wdl4* lines at 4 and 6 dpg also revealed no significant differences (Supplemental Fig. S3).

Treatment with exogenous auxin induces transverse microtubule array patterning in hypocotyl cells on a 2 h time course (Vineyard et al. 2013, Elliott and Shaw 2018). We used this functional assay to determine if the cortical arrays were aberrant for the dynamic process of reorganization. Incubation for 2 h with the synthetic auxin, picloram (5 μM), correctly induced transverse microtubule array patterns in all 3 genetic backgrounds (Fig. 4, D to F). Comparing wild type to *wdl4* seedlings, we observed no significant difference ($P > 0.05$, rank sum tests of normalized counts) in the percentages of transverse array patterns and a very modest difference ($P = 0.05$) for 35s:WDL4 (Fig. 4G), indicating that loss or constitutive expression of *WDL4* does not block or substantially delay the cell's ability to form transverse array patterns.

Hypocotyl growth induction by phytohormones

WDL4 is upregulated by auxin (Chapman et al. 2012) and responsive to ethylene levels (Deng et al. 2021). These phytohormones, together with BRs, have overlapping and interdependent effects on hypocotyl growth (Vandenbussche et al. 2005, Verma et al. 2016). Exogenous application of these hormones promotes concentration-dependent hyperelongation of hypocotyls under light-grown conditions (Li et al. 1996, Collett et al. 2000, Yu et al. 2013). To determine if loss of WDL4 function alters hormone growth response, we treated seedlings with exogenous auxin (via picloram), BR (via epibrassinolide), or ethylene (via 1-aminocyclopropane-1-carboxylate [ACC]) and measured hypocotyl length.

We treated 3 dpg seedlings with 1 μM, 5 μM, or 10 μM picloram, for 3 d under lighted conditions and measured hypocotyl length at 6 dpg (Fig. 5A). Wild-type, *wdl4*, and *35s:WDL4* seedlings exhibited the same general pattern of hypocotyl growth response, increasing length at 1 μM and 5 μM before showing a reduced response at 10 μM (Fig. 5A; Supplemental Fig. S4A). These data show that auxin induces additional growth in *wdl4*, albeit not to the same magnitude as wild type or *35s:WDL4*, and that the peak auxin concentration for growth induction is not substantially different between wild type, *wdl4*, or *35s:WDL4* lines under these conditions.

BR acts in concert with auxin to induce hypocotyl elongation (Oh et al. 2014). At 6 dpg we observed a mostly proportional response to 0.1 μM, 1.0 μM, and 10 μM exogenous BR after the 3-d treatment period (Fig. 5B; Supplemental Fig. S4B). At the highest concentration, BR induced substantially more axial growth than observed with auxin induction in all genotypes. Induction of 35s:WDL4 lines with 10 μM BR resulted in less hypocotyl extension than observed in wild type ($P < 0.05$), consistent with dark-growth measurements.

Ethylene induced hypocotyl extension under light-grown conditions in wild-type hypocotyls as assayed by growth on 0.1 μM, 1.0 μM, and 10 μM ACC (Fig. 5C). Wild-type

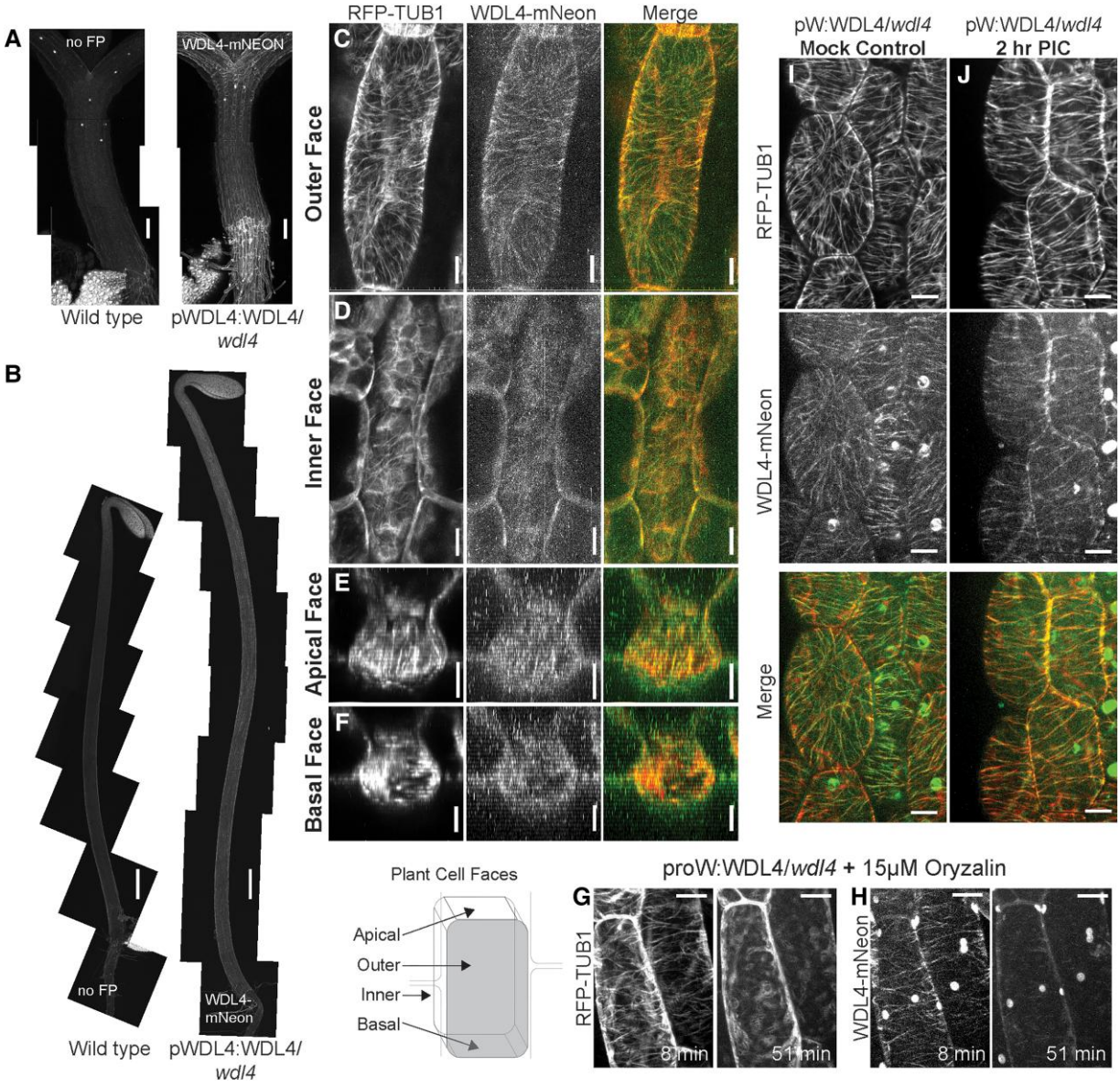

Figure 3. WDL4 colocalizes will microtubules in hypocotyl cells. **A)** Stitched maximum projection image from 5 dpg control seedlings (no fluorescent protein) and *pWDL4:WDL4-mNeon* grown in 24 h light exhibiting expression in all epidermal hypocotyl cells. Bar = 100 μm. Stitched maximum projection images of control **B)** and *pWDL4:WDL4-mNeon* hypocotyls for dark-grown seedlings at 5 dpg indicated WDL4-mNeon accumulation in all epidermal cells regardless of light treatment. Bar = 500 μm. **C to J)** Representative images of 5 dpg hypocotyl cells coexpressing 35s:RFP-TUB1 and pWDL4-WDL4:mNeon. Colocalization was observed on the outer periclinal cell face **C)**, the inner periclinal cell face **D)** scale bar = 10 μm, and the anticlinal apical and basal cell faces **E and F)** scale bar = 5 and 3 μm, respectively (see diagram for cell face designation). Treatment with the microtubule inhibitor, oryzalin, of *wdl4* hypocotyls coexpressing 35s:RFP-TUB1 **G)** and proW:WDL4-mNeon **H)** indicates concurrent loss of microtubules and WDL4 cortical localization by 51 min. Bar = 10 μm. WDL4-mNeon remains associated with cortical microtubules after induction of transverse array patterns with auxin analog, picloram **I and J)**. Bar = 10 μm.

seedlings showed a graded response, reaching 110%, 129%, and 167% of untreated hypocotyl length and exhibited epinastic cotyledons after 6 d (Supplemental Figs. S4C and S5A). *wdl4* seedlings showed no measurable increase in hypocotyl length at 0.1 μM, 1.0 μM, or 10 μM ACC under the same conditions (Fig. 5C, $P > 0.05$) but exhibited epinastic cotyledons, indicating ACC perception (Supplemental Fig. S5B). ACC treatment of 35s:WDL4 seedlings increased hypocotyl length at 0.1 μM, 1.0 μM, but the response was attenuated at 10 μM ($P < 0.5$) compared to controls (Fig. 5C; Supplemental Fig. S5C). These data indicate that WDL4 increases ethylene sensitivity with respect to hypocotyl growth induction.

Hypocotyl elongation is driven, in part, by cell wall acidification (i.e. acid growth) through induction of a plasma membrane H^+ ATPases (Spartz et al. 2012, Takahashi et al. 2012).

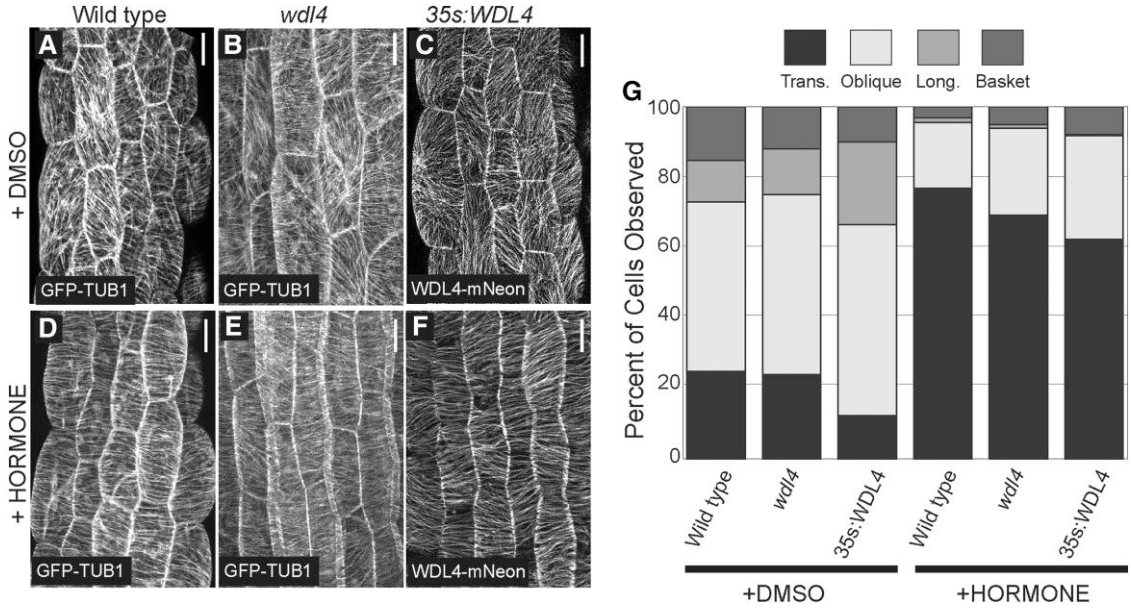

Figure 4. Cortical microtubule arrays form the correct patterns in the wdl4 mutant. Confocal imaging of wild type **A)** and *wdl4* **B)** epidermal hypocotyl cells expressing GFP:TUB1 and wild type constitutively expressing WDL4:mNeon **C)** under light-grown conditions at 22 °C after 2 h control treatment (+DMSO). Wild-type **D)**, *wdl4* **E)**, and constitutive WDL4 expression **F)** after 2 h treatment with 5 μM picloram, an auxin analog (+HORMONE), indicating correct reorganization to transverse coalignment. Scale bar = 20 μm **G)** Bar graphs indicating the percentage of cells showing transverse (trans.), oblique, longitudinal (long.), and basket array patterns after 2 h control (+DMSO) and 5 μM picloram (+HORMONE) treatments in continuous light at 22 °C. Percentage taken from all cells in at least 2 adjacent cell files for each of 5 seedlings per treatment for wild type, *wdl4*, and seedlings constitutively expressing WDL4:mNeon. Rank sum tests of percentages per seedling indicate no significant difference for wild type vs *wdl4* and ($P > 0.05$) and a significant difference ($P \leq 0.05$) for wild type vs 35s:WDL4 for transverse patterns in mock and hormone treated experiments.

To evaluate the possibility that WDL4 might directly alter ATPase function or cell wall extensibility, seedlings were transferred to plates containing 5 μM fusicoccin, a fungal toxin that activates plasma membrane H^+ ATPases. Wild-type hypocotyls exposed to fusicoccin from days 4 to 6 dpg were ∼240% of wild-type controls (Fig. 5D). Measurements of *wdl4* or 35s:WDL4 seedlings showed average increases of hypocotyl length to 210% and 230% of untreated, respectively. We interpret these results to be of similar magnitudes of effect, suggesting that the *wdl4* hyper-elongation phenotype is unlikely to arise because of H + ATPase deficiencies or differences in cell wall materials that result in persistent axial growth after 4 dpg.

WDL4 modulates cell elongation at elevated temperatures

Hypocotyls hyper-elongate in response to elevated ambient temperature, a response to environmental change that depends upon auxin signaling (Gray et al. 1998) and occurs during elevated ethylene production (Smalle et al. 1997, Poór et al. 2022). To evaluate temperature effects on *wdl4*, we germinated seedlings at 22 °C for 24 h under continuous light and either maintained seedlings at 22 °C (control) or shifted plants to 28 °C from 3 to 5 dpg before hypocotyl measurement (Fig. 6, A to D). In agreement with prior studies (Gray et al. 1998), 28 °C increased wild-type hypocotyl length to ∼200% (Fig. 6, E and F) of 22 °C controls (e.g. 22 °C 0.67 ± 0.17 mm vs 28 °C treated 1.19 ± 0.33 mm, at 24 h of treatment). Comparing *wdl4* at 22 °C and 28 °C (Fig. 6, G and H), we observed a dramatic increase in hypocotyl length, ranging from 350% after 24 h of heat treatment, to nearly 500% after 72 h. Comparing wild-type seedlings to *wdl4* at 28 °C, we observed a 550% increase in hypocotyl length by 5 dpg (Fig. 6F and H). These results show that WDL4 plays an outsized role in suppressing axial hypocotyl cell elongation in response to ambient temperature.

To determine if the *wdl4* temperature response lies outside of the auxin-dependent pathway, we crossed *wdl4* to the *axr2-1* dominant auxin coreceptor mutant (Wilson et al. 1990). Control experiments, comparing hypocotyl length for *axr2-1* grown at 22° and 28 °C at 3 to 5 dpg (Fig. 6, I and J), recapitulated prior results showing a 140% increase for *axr2-1* at the higher temperature (Reed et al. 2018). Measurements of *axr2-1* and *wdl4/axr2-1* at 22 °C were not significantly different (Fig. 6I, K and Q) (2-tailed t-test, $P > 0.05$ at 5 dpg), indicating suppression of the *wdl4* hyper-elongation phenotype by the *axr2-1* dominant mutant. At 28 °C, the *wdl4/axr2-1* double mutant showed a nearly complete suppression of the *wdl4* hyper-elongation phenotype (Fig. 6H and L). Consistent with results for *axr2-1*, *wdl4/axr2-1* hypocotyls grown at 28 °C were 140% longer than control double mutants grown at 22 °C (Fig. 6, K and L). Examining the ratio of average hypocotyl lengths at 22° and

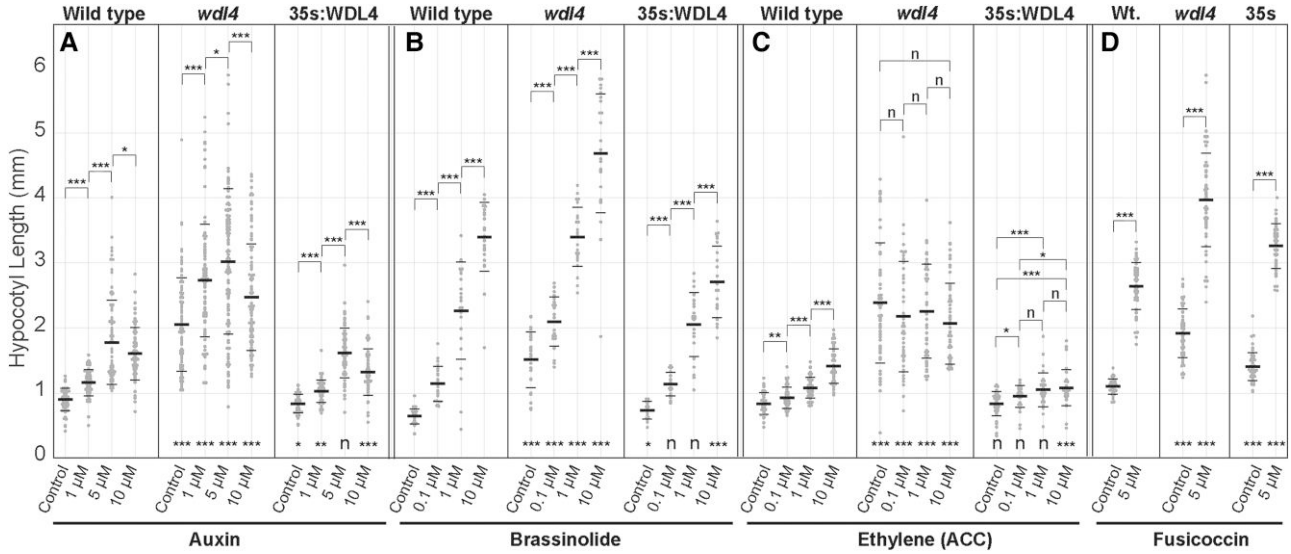

Figure 5. Growth response to exogenous hormone treatments and fusicoccin. Evaluation of hypocotyl length after growth at 22 °C in continuous light on agar plates supplemented with **A)** auxin, **B)** BR, **C)** ACC (ethylene), or **D)** fusicoccin. Gray dots are individual plants, heavy bar is mean, and lighter bars are standard deviation. **A)** Growth from days 4 to 6 postgermination on a concentration series of the light-stable synthetic auxin, picloram, indicated maximum effect at or above 5 µM for wild type, *wdl4*, and the 35s:WDL4 constitutively expressing seedlings ($n > 47$ seedlings). **B)** Growth from days 4 to 6 postgermination on a BR (epibrassinolide) log10 concentration series produced a roughly linear increase in hypocotyl length for wild type, *wdl4*, and 35s:WDL4 seedlings with 35s:WDL4 less responsive at the highest concentration compared to wild type (10 µM, t-test $P = < 0.01$, $n > 20$). **C)** Growth from days 2 to 6 postgermination on concentration series of ACC increased wild-type hypocotyl length to a maximum of 150% of control but did not increase *wdl4* hypocotyl length at 10 µM (t-test $P = 0.83$, $n > 37$). The ACC growth induction was somewhat less effective on 35s:WDL4 seedlings at 10 µM (t-test $P = 0.1$, $n > 20$) versus control when compared to wild type. **D)** The fungal peptide, fusicoccin, at 5 µM in liquid culture from days 4 to 6, induced hypocotyl elongation to ~220% of untreated seedlings for wild type, *wdl4*, and 35s:WDL4 backgrounds indicating a proportional effect on growth for all lines with persistent cell wall acidification. *P*-values are derived from 2-tailed t-test comparing the same age wild type (below data plots) or between bracketed treatments (above data plots). $^*P < 0.05$, $^{**}P < 0.001$, $^{***}P < 0.0001$, n = not significant.

28 °C (Fig. 6M to P) indicated that the block to temperature-dependent hyper-elongation in the *axr2-1* background is extended to the *axr2-1/wdl4* double mutant, indicating genetic control of the growth phenotype beyond mechanical or physiological changes associated with elevated temperature.

To further probe the specific requirement for auxin signaling in the *wdl4* phenotype, we treated light-grown seedlings with 10 µM auxinole, a synthetic antagonist that directly inhibits TIR1 activity (Hayashi et al. 2012). Seedlings were treated at 3 dpg and either kept at 22 °C or moved to high temperature (28 °C) for 3 d prior to growth measurements at 6 dpg. At 22 °C, both wild type and constitutive 35s:WDL4 seedlings had no significant change ($P > 0.05$) in hypocotyl length (Supplemental Fig. S6). In contrast, auxinole treatment reduced *wdl4* hypocotyl length to 68% of untreated controls ($P = 0.015$) (Supplemental Fig. S6). At 28 °C, auxinole significantly reduced hypocotyl elongation in all genotypes. Wild-type and 35s:WDL4 hypocotyl elongation at 28 °C were reduced to 55% and 48% of controls, respectively ($P << 0.001$). *wdl4* seedlings grown at 28 °C with auxinole grew to 74% of untreated ($P = 0.019$), indicating a smaller effect than with wild type (Supplemental Fig. S6). These data suggest that auxin plays an important role in stimulating axial elongation but is not exclusively responsible for the *wdl4* hyper-elongation phenotype at 22 or 28 °C.

WDL4 plays a role in the ethylene-dependent unhooking of the hypocotyl (Deng et al. 2021), and ethylene production is upregulated at elevated temperatures (Smalle et al. 1997, Poór et al. 2022). We also observed that *wdl4* seedlings at 22 °C responded in a similar pattern to auxin and BR concentrations but ACC failed to elicit additional hypocotyl growth (Fig. 5). We, therefore, asked if *wdl4* remained insensitive to ethylene when grown at 28 °C (Fig. 6R to T). Measurements of wild-type hypocotyls at 6 dpg showed that ACC significantly increased length at 0.1 µM and 1 µM ($P < 0.001$; $n > 50$) but had no effect at 10 µM ($P = 0.75$) in these assays. In contrast, *wdl4* trended shorter at 0.1 µM ACC ($P > 0.05$) and showed a dramatic response to higher ACC concentrations, effectively blocking temperature-dependent hyper-elongation at 10 µM ($P << 0.001$) (Fig. 6R; Supplemental Fig. S4D). Plants constitutively expressing WDL4 responded similarly to wild type with a small length increase at 0.1 µM ACC and no effect at higher concentrations ($P > 0.05$) (Fig. 6T; Supplemental Fig. S6D). These results show that the temperature-dependent *wdl4* hyper-elongation is suppressed with elevated ethylene levels and

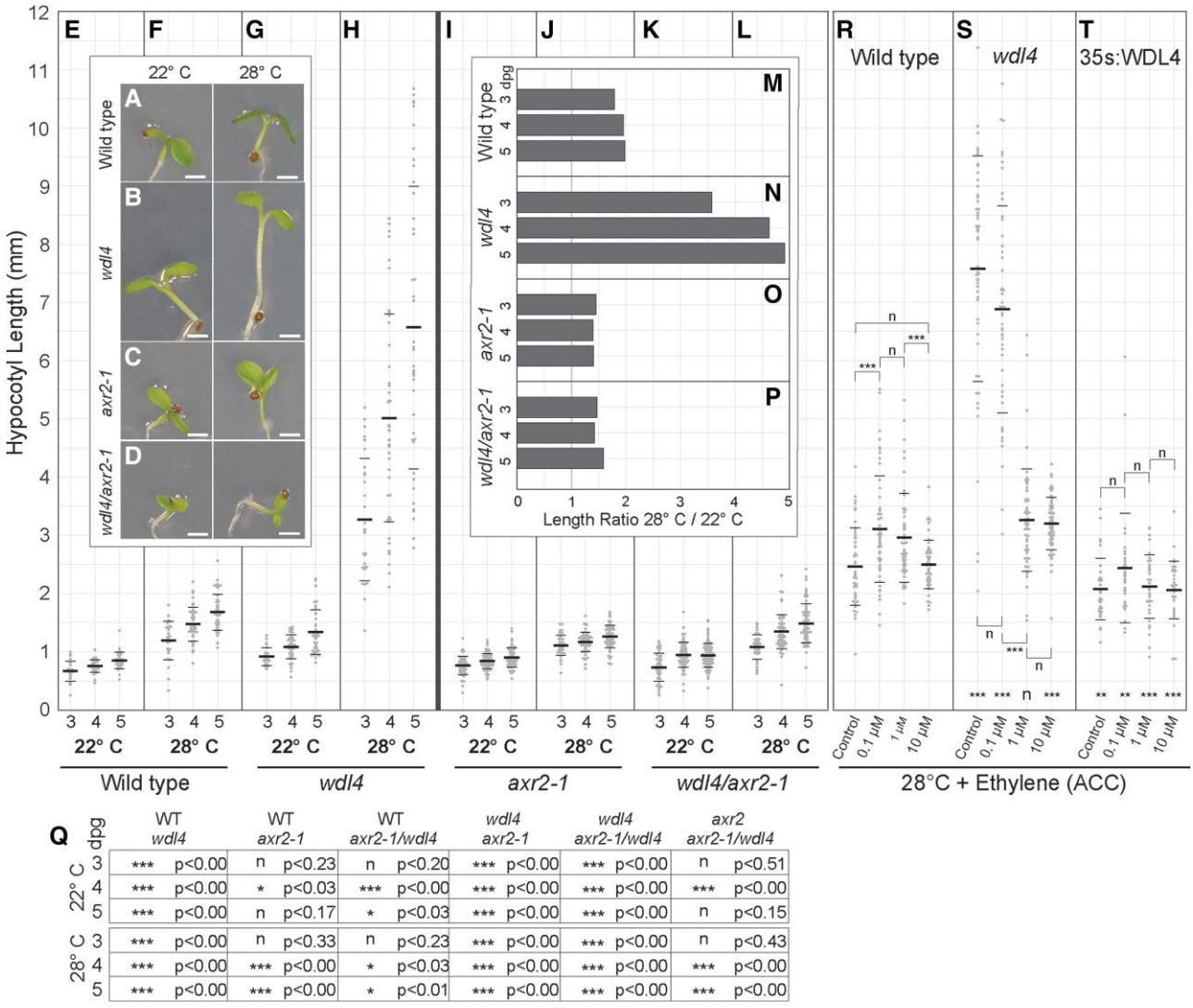

Q

dpg	WT *wdl4*	WT *axr2-1*	WT *axr2-1/wdl4*	*wdl4* *axr2-1*	*wdl4* *axr2-1/wdl4*	*axr2* *axr2-1/wdl4*
22° C 3	*** p<0.00	n p<0.23	n p<0.20	*** p<0.00	*** p<0.00	n p<0.51
22° C 4	*** p<0.00	* p<0.03	*** p<0.00	*** p<0.00	*** p<0.00	*** p<0.00
22° C 5	*** p<0.00	n p<0.17	* p<0.03	*** p<0.00	*** p<0.00	n p<0.15
28° C 3	*** p<0.00	n p<0.33	n p<0.23	*** p<0.00	*** p<0.00	n p<0.43
28° C 4	*** p<0.00	*** p<0.00	* p<0.03	*** p<0.00	*** p<0.00	*** p<0.00
28° C 5	*** p<0.00	*** p<0.00	* p<0.01	*** p<0.00	*** p<0.00	*** p<0.00

Figure 6. Elevated temperature exacerbates *wdl4* elongation phenotype and is suppressed by the *axr2-1* dominant auxin receptor mutant and ethylene. Representative images of wild type **A)**, *wdl4* **B)**, *axr2-1* **C)**, and the *wdl4*/*axr2-1* double mutant **D)** at 5 dpg grown in continuous light at 22 °C or 28 °C (bar = 1 mm). Hypocotyl measurements made at 3, 4, and 5 dpg for wild type at 22 °C **E)** and 28 °C **F)**, *wdl4* at 22 °C **G)** and 28 °C **H)**, *axr2-1* at 22 °C **I)** and 28 °C **J)**, and the *wdl4*/*axr2-1* double mutant at 22 °C **K)**, and 28 °C **L)** indicating effects of elevated temperature on seedling growth and suppression of hypocotyl hyper-elongation in the *axr2-1* mutant background. Dots represent individual seedlings, thick bar is mean value, and thin bars are standard deviation. Ratio of hypocotyl lengths from plants grown under 28 °C versus 22 °C conditions indicating a 2-fold increase in length for wild type **M)**, 3.5- to 5-fold increase for *wdl4* **N)**, and a 1.5-fold increase for both the *axr2-1* **O)** and *wdl4*/*axr2-1* **P)** double mutant lines. Table of 2-tailed t-tests **Q)** for data sets in E-L. Hypocotyl length at 28 °C at 5 dpg for wild type **R)**, *wdl4* **S)**, and the 35s:WDL4 **T)** lines on increasing concentrations of ACC indicating suppression of temperature-induced hyper-elongation by ethylene. *P*-values are derived from 2-tailed t-test comparing the same age wild type (below data plots) or between bracketed treatments (above data plots) **R to T)**. For all *P*-values $^{*}P < 0.05$, $^{**}P < 0.001$, $^{***}P < 0.0001$, *n* = nonsignificant.

that ethylene sensitivity related to axial growth has been shifted in *wdl4*.

The DR5 auxin transcriptional reporter is attenuated in hyper-elongated *wdl4* hypocotyls

WDL4 is strongly upregulated by auxin in hypocotyls (Chapman et al. 2012), and we found that the *wdl4* hyper-elongation phenotype was suppressed both in the *axr2-1*/*wdl4* double mutant and with auxinole treatment. We, therefore, hypothesized that *wdl4* hyper-elongation after 4 dpg could arise from elevated or persistent auxin activity in light-grown seedlings. To investigate this hypothesis, we crossed the DR5:GFP auxin-sensitive transcriptional reporter (Ulmasov et al. 1997) into *wdl4* and used LSCM to assess reporter expression at 3 dpg, when both wild type and *wdl4* show hypocotyl elongation, and at 5 dpg after wild type arrests growth and *wdl4* is still elongating (Fig. 7). The spatial distribution of DR5:GFP signal in wild-type hypocotyls exhibited 2 distinct features at both 3 and 5 dpg including an

asymmetrically distributed fluorescence in the upper half and a central longitudinal midline fluorescence in the lower half (Fig. 7, A and B). We observed asymmetric DR5:GFP signal in the upper half of *wdl4* seedlings but found little evidence for lower midline signal at 3 or 5 dpg (Fig. 7, D and E) suggesting a specific loss of auxin-dependent gene expression in the basal half of *wdl4* hypocotyls.

To quantitatively compare DR5:GFP signal between wild type and *wdl4*, we divided the hypocotyl into 5 equally spaced longitudinal zones (Fig. 7G) from base (zone 5) to apex (zone 1) and determined the mean pixel value per zone after subtraction of no-GFP control plants from the same slide (see Methods). Tabulated *P*-values from 2-tailed t-tests (Fig. 7G) indicated no significant difference between wild type and *wdl4* at 3 dpg. At 5 dpg, and contrary to our hypothesis, the *wdl4* plants trended lower than *wdl4* at 3 dpg, showing no significant difference in DR5:GFP signal. Wild-type hypocotyls at 5 dpg showed significantly elevated DR5:GFP levels across all but one zone, when compared to *wdl4*, and trended higher compared to wild type at 3 dpg. Taken together, these observations indicate that *wdl4* hyper-elongation at 5 dpg does not coincide with an increase in auxin-dependent DR5:GFP signal.

To determine the relative contributions from asymmetric and midline DR5:GFP features, seedlings were oriented with the higher asymmetric signal on the left and the average longitudinal DR5:GFP intensity for each zone was determined to create the transverse intensity distribution (Fig. 7H and diagram). Comparing wild type and *wdl4* at 3 dpg, we observed similar distributions of asymmetric signal in the 2 apical zones (1 and 2) with more signal in zone 3 for *wdl4* and no distinct midline fluorescence for *wdl4* compared to wild type (Fig. 7I; Supplemental Fig. S7A). Comparisons at 5 dpg showed the asymmetric signal extending further down the hypocotyl (zones 1 to 3) in both wild type and *wdl4* (Fig. 7H, middle panels; Supplemental Fig. S7B). The midline signal was elevated in 5 dpg wild-type hypocotyls that should be arrested for growth, increasing toward the hypocotyl base. Midline signal was just detectable in *wdl4* hypocotyls for zone 5 (Fig. 7H; Supplemental Fig. S7B). These data show that the increased DR5:GFP signal in wild type plants from 3 to 5 dpg was due primarily to increased midline expression where *wdl4* plants appeared attenuated for total signal with almost no midline signal detected at 3 or 5 dpg.

Growth at 28 °C produced a 500% increase in *wdl4* hypocotyl length when compared with wild-type plants (Fig. 5), a phenotype that was blocked by the dominant *axr2-1* auxin coreceptor mutant and attenuated by auxinole treatment. We reasoned that if elevated auxin levels, or a change in auxin trafficking, were driving hyper-elongation, we would observe elevated DR5:GFP expression in the *wdl4* hypocotyl when grown at 28 °C. We observed that DR5:GFP signal in wild-type 28 °C plants at 5 dpg was visibly higher in cotyledons (Fig. 7C) with hypocotyl DR5:GFP signal trending higher when compared to 22 °C (Fig. 7G). Hyper-elongating 28 °C *wdl4* seedlings (Fig. 7F) did not exhibit increased DR5:GFP signal, trending lower relative to 22 °C, with no observed signal asymmetry in the apical region and trace indication of midline signal (Fig. 7H, right bottom panel; Supplemental Fig. S7C). These data provide additional evidence that despite the auxin requirement for hyper-elongation indicated from *axr2-1*/*wdl4* and auxinole experiments, the growth phenotype does not coincide with elevated levels of DR5:GFP reporter to indicate a regional increase in auxin-dependent gene expression.

Discussion

The role of microtubules in cellular morphogenesis

Plants control cell expansion by manipulating the chemical properties of the cell wall. In the best described molecular mechanism, auxin activates plasma membrane proton pumps through a TIR1/AFB transcriptional pathway (Spartz et al. 2012, Friml 2022). The resulting acidification results in wall extension against the stress of turgor pressure producing irreversible cell growth (Cosgrove 2005, Braidwood et al. 2014). Eliminating microtubules prevents hypocotyl cells from achieving a correct shape but does not directly alter the capacity of the plant cell to expand (Braidwood et al. 2014). Hence, microtubules influence plant cell shape through effects on cellulose deposition but have no known direct role in cell size control. Our data, together with work examining the role of WDL4 in apical hook opening (Deng et al. 2021), provide evidence that this microtubule associated protein plays a key role in modulating cell size in axially extending hypocotyl cells without altering microtubule patterning, suggesting an unconventional role for microtubule associated proteins.

WDL4 controls hypocotyl cell size and not cell shape determination

Our investigation of WDL4 found a light-dependent hyper-elongation phenotype for the *wdl4* loss of function mutant, with no evidence for cell swelling, twisting, or morphological defects related to a loss of growth anisotropy typically associated with defects in cortical array patterning. *wdl4* cell length followed the established pattern for etiolated hypocotyls, where cells taper from longer to shorter in a basal to apical gradient. The *wdl4* hyper-elongation accrued primarily through a continuation of axial cell growth, continuing elongation beyond 4 dpg, when wild-type plants arrested. WDL4, therefore, appears to control when the cell elongates more than changing the rate of cell elongation in light-grown hypocotyls. The extended growth period was not accompanied by a developmental delay, as evidenced by leaf emergence at the apical meristem. Finally, the response to fusicoccin suggested that the cell wall materials were responding similarly to wild-type plants for acid-induced cell growth and not aberrantly to produce the hyper-elongation. These data indicate that WDL4 functions in cell size control and does not directly affect cell shape in the context of losing cellular growth anisotropy.

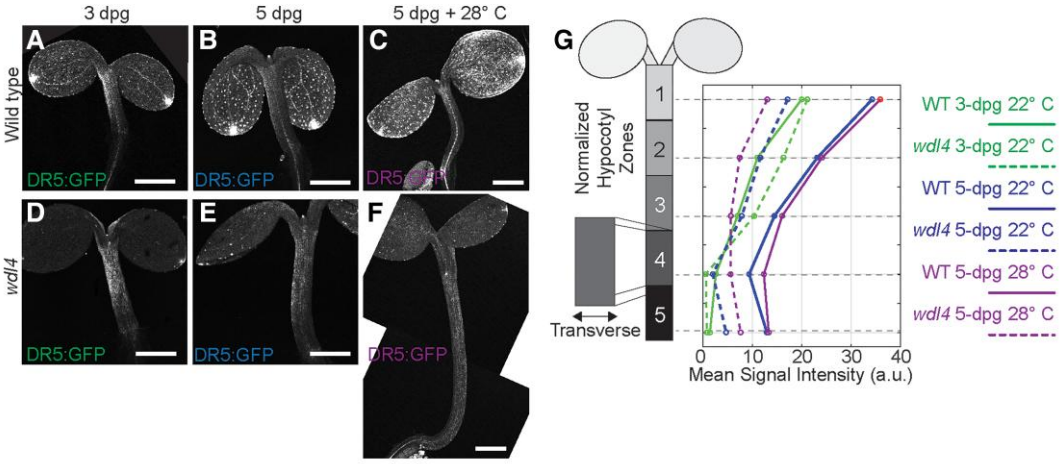

t-Test p-Values

Zone	WT3d22° mt3d22°	WT5d22° mt5d22°	WT5d28° mt5d28°	WT3d22° WT5d22°	WT5d22° WT5d28°	WT3d22° WT5d28°	mt3d22° mt5d22°	mt5d22° mt5d28°	mt3d22° mt5d28°
1	0.8924	**0.0072**	**0.0011**	0.1442	0.8310	0.0507	0.5257	0.4065	0.2392
2	0.4797	**0.0318**	**0.0005**	0.1470	0.8813	**0.0279**	0.3904	0.2840	0.1174
3	0.6211	0.1443	**0.0056**	0.2983	0.7668	0.0546	0.5920	0.5350	0.3778
4	0.6373	**0.0244**	**0.0101**	0.1910	0.4297	**0.0037**	0.6400	0.1530	0.1532
5	0.8732	**0.0209**	**0.0179**	**0.0329**	0.9227	**0.0008**	0.2695	0.2788	**0.0148**

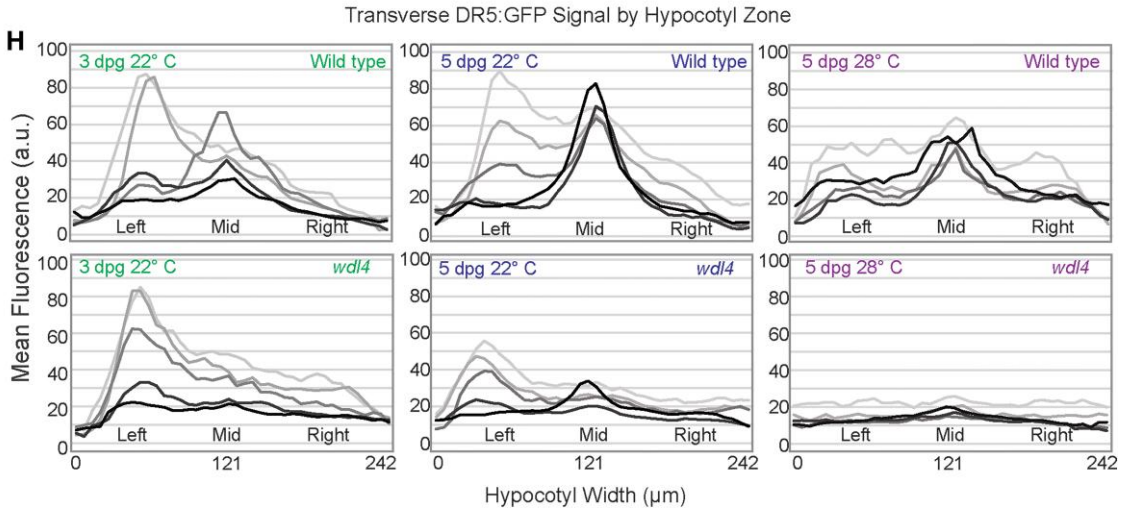

Figure 7. Spatial distribution of auxin-dependent DR5:GFP expression in wdl4 hypocotyls. Confocal z-series projections of wild type **A to C)** and *wdl4* **D to E)** and composite *wdl4* **F)** seedlings expressing an auxin-dependent DR5:GFP transcriptional reporter under different conditions. Wild-type DR5:GFP signal in growing 3 dpg light-grown 22 °C hypocotyls was observed prominently as an apical lateral gradient and a basal midline signal **A)**. The apical DR5:GFP gradient was also observed in 3 dpg *wdl4* hypocotyls, but no signal was observed in the basal *wdl4* hypocotyl midline **D)**. By 5 dpg, growth-arrested wild-type hypocotyls exhibited increased DR5:GFP signal in both apical and basal regions, **B)** whereas hyper-elongating 5 dpg *wdl4* hypocotyls **E)** maintained similar DR5:GFP levels over the lateral apical gradient and no visible basal midline signal. Growth at 28 °C resulted in mildly elevated wild-type signal **C)** with no apparent signal elevation for *wdl4* hypocotyls **F)**. Averaged DR5:GFP fluorescence signal from 5 equipartitioned hypocotyl zones **G)** after subtraction of no-GFP controls for all conditions in **A** to **F**) with *P*-values for all comparisons as indicated (2-tailed t-tests, $N = 9$ WT3dpg22°, 9 MT3dpg22°, 26 WT5dpg22°, 25 MT3dpg22°, 16 WT3dpg28°, 13 MT3dpg28°, bold indicates significance $P < 0.05$). Averaged transverse signal value across hypocotyl zones **H)** using zone color designation from **G)**. Values represent mean signal across each zone with seedlings oriented to have higher apical gradient to left side.

WDL4 associates with cortical microtubules

We quantitatively assessed the distribution of microtubule array pattern types in both light-grown and hormone-induced *wdl4* hypocotyls and found no compelling evidence for patterning defects or increased transverse array frequency as would be predicted for mutations leading to more axial elongation. The possibility that WDL4, a TPX2-domain protein, impacts microtubule array dynamics through microtubule nucleation was strongly discounted by our observation that *wdl4* plants had the same density of growing microtubule plus ends and the same polymerization velocity as wild-type cells. Moreover, auxin treatment resulted

in the correct reorientation of polymers to a transverse coalignment at 2 h (Vineyard et al. 2013), a functional test for both gain of transverse and loss of longitudinal polymers (Thoms et al. 2018). These negative data for the loss of function *wdl4* mutant cannot completely rule out a possible role in modifying array pattern but are consistent with the absence of morphological cell shape defects related to cell wall anisotropy.

Constitutive WDL4 expression had a limited effect on array pattern distribution but no clear effect on axial growth at 22 °C. Constitutive WDL4 lines significantly retarded etiolated hypocotyl growth, but without producing gross morphological defects, again indicating an effect on cell size rather than cell shape. Hence, we find no direct evidence linking the action of WDL4 on microtubules to the hyper-elongation to suggest a causal connection. These data, together with observations made for WDL4 retarding apical hook opening (Deng et al. 2021), indicate that this microtubule associated protein plays a role in controlling cell size without appearing to modify the array patterns.

Potential roles for microtubule-associated proteins in growth control

Cortical microtubules are anchored to the plasma membrane (Shaw et al. 2003), providing an attachment point for molecules and vesicles moving in the streaming cytoplasm. We found WDL4 was associated with all cortical microtubule populations, under all tested conditions, suggesting a general role at the cell cortex. Recent in vitro experiments (Fujiwara et al. 2014, Deng et al. 2021) showed WDL4 interacting with several syntaxin proteins, including SYNTAXIN OF PLANTS (SYP)121/PENETRATION (PEN)1, SYP122, SYP21/PEP12, and SYP43. SYP121/PEN1 and SYP122 facilitate exocytosis, including cell wall materials (Waghmare et al. 2018), and SYP121/PEN1 directly interacts with the Rho-GTPase, ROP2, to promote vesicle trafficking during root-tip growth (Cui et al. 2022). SYP43 localizes to the trans-Golgi network (Sanderfoot et al. 2001) and functions in vesicle recycling (Uemura et al. 2012). These data suggest that WDL4 could be using the microtubule cytoskeleton to mediate vesicle interactions with the plasma membrane or endoplasmic reticulum. The absence of gross cell shape defects in general or after fusicoccin treatment discounts a role for WDL4 in organizing the deposition of cell wall materials for anisotropic growth. However, WDL4 could function in distributing other polysaccharides, signaling molecules, transporters, receptors, or ATPases in the plasma membrane involved with cell size control (Cosgrove 2022).

WDL4 and the control of axial growth by phytohormones

Arabidopsis Col-0 hypocotyls under lighted laboratory conditions grow slowly to around 1 mm at 22 °C by 4 dpg before arresting growth and awaiting emergence of the first true leaves at 6 to 7 dpg. In this time-period between 4 and 6 dpg, hypocotyls can be stimulated to rapidly elongate by environmental cues such as unilateral light, shade, or ambient temperature. This "hyper-elongation" beyond 1 mm is also elicited using exogenous auxin, BR, or ethylene (Li et al. 1996, Collett et al. 2000, Yu et al. 2013) and is genetically blocked by the dominant *axr2-1* auxin coreceptor mutant (Gray et al. 1998, True and Shaw 2020). The *wdl4* hyper-elongation phenotype resembles the effects of exogenous auxin or ethylene treatment at 22 °C where hypocotyls continue elongation after 4 dpg to about 2 mm (True and Shaw 2020). These data, and the auxinole experiments, suggest that WDL4 could negatively regulate this later phase of hypocotyl growth through changes to phytohormone distribution or sensitivity.

Auxin plays a critical role in hypocotyl growth in part because it can be redistributed into lateral and longitudinal gradients as it flows basipetally from the apical meristem (Friml 2022). Auxin production is also upregulated at elevated temperatures, potentially driving the hyper-elongation observed under these conditions (Gray et al. 1998). We speculated that because auxin upregulates WDL4 in the hypocotyl (Chapman et al. 2012), WDL4 could be a negative feedback on auxin-induced growth to structure or condition hormone response. To examine this hypothesis, we determined the effects of exogenous auxin on hypocotyl growth, examined growth at elevated temperature when auxin production increases, and evaluated the spatial extent of auxin-dependent gene expression using the DR5:GFP reporter. We expected that if the *wdl4* hyper-elongation at 22 and 28 °C was driven by elevated auxin levels or sensitivity, as suggested by *axr2-1*/*wdl4* and auxinole results, we would observe a change in sensitivity to exogenous auxin and auxinole in growth assays and increased DR5:GFP reporter signal. Our experiments showed that the peak auxin concentration for growth induction, before reaching the threshold to growth retardation, was not shifted in *wdl4* when compared to wild type, suggesting that *wdl4* plants are not hyper-elongating solely due to altered endogenous auxin levels or hyper-sensitivity. We additionally found that auxin treatments of *wdl4* at 22 °C could not replicate the extreme (i.e. 5-fold) hyper-elongation observed at 28 °C, suggesting a requirement for more than elevated auxin. We observed no increase in auxin-dependent DR5:GFP reporter signal at the *wdl4* hypocotyl apex to suggest that elevated auxin response drives the cell elongation. Oppositely, we found that the signal actually decreased in large part, because the *wdl4* plants showed almost no DR5:GFP signal at the midline toward the hypocotyl base. Together, these data do not support the hypothesis that WDL4 is acting directly or solely through auxin signaling to retard axial growth but provide limited evidence that WDL4 can affect where auxin-dependent gene expression occurs in the hypocotyl.

Ethylene is an important regulator of hypocotyl elongation in the dark when seedlings suppress hook opening (i.e. axial growth) in the apical region while driving axial extension further down the hypocotyl to bring the cotyledons out of the

soil. Ethylene also plays a significant general role in plant stress responses, including heat stress (Poór et al. 2022). Recent data show that ethylene promotes hypocotyl growth at lower concentrations and inhibits growth at higher concentrations, similar to auxin (Smalle et al. 1997). Ethylene treatment additionally impacts auxin production through an EIN3-dependent pathway (Vandenbussche et al. 2010). These observations led us to hypothesize that the *wdl4* hyper-elongation could come about if WDL4 normally modulates the cellular growth response to ethylene. Unlike auxin and BR, *wdl4* plants showed a marked change in sensitivity to ACC, conditioned by temperature. Wild-type hypocotyls were stimulated to elongate with 0.1 µM ACC where *wdl4* seedlings did not respond.

Wild-type hypocotyls at 28 °C, where ethylene production increases, increased length at 1 µM ACC before showing retardation at 10 µM ACC. In contrast, 0.1 µM ACC did not elicit growth in *wdl4* seedlings at 28 °C, where 1 µM and 10 µM ACC dramatically retarded growth. Consistent with these observations, 35s:WDL4 seedlings exhibited the same growth responses to ACC as wild type at 22° and 28 °C, but the magnitude of the response was reduced across all concentrations. Last, constitutive WDL4 expression substantially impeded growth in dark-grown, etiolated seedlings where ethylene is high (Liang et al. 2012, Yu et al. 2013). We interpret these observations to show that ethylene acts on wild type and *wdl4* in the same capacity, but the peak concentration of ethylene required to promote or retard growth in *wdl4* has been shifted. WDL4 appears to suppress the action of ethylene on hypocotyl cell growth.

In sum, WDL4 is responsible for limiting axial hypocotyl growth in light grown seedlings and plays an outsized role in responding to elevated ambient temperatures. WDL4 was previously shown to retard apical hook closure in the dark, a form of differential axial growth (Deng et al. 2021). The prior work described ethylene regulatory sites in the WDL4 promoter and suggested a role for WDL4 in controlling auxin distribution (Deng et al. 2021). In partial agreement with that work, we observed that *wdl4* mutants were more ethylene sensitive, in the form of ACC treatment, for axial growth and showed distinct spatial differences in auxin-dependent reporter distribution. We, however, found no direct evidence for auxin hyper-sensitivity. Extending prior findings, we observed continuous WDL4 association with cortical microtubules throughout hypocotyl development and found no measurable difference in cortical array patterning for the loss of function *wdl4* correlated with hypocotyl hyper-elongation. Constitutive WDL4-mNEON expression in the wild-type background led to shorter dark-grown hypocotyls and a measurable increase in transverse array patterning suggesting that WDL4 could play some role in cortical patterning or that the signaling effect of WDL4 on growth retardation is upstream of signaling for transverse array patterning. Noting the loss-of-function growth phenotype and results reported for WDL4 in apical hook retardation that also failed to find evidence of effects on array patterning (Deng et al. 2021), we propose that WDL4 uses the microtubules as a platform for affecting how these axially growing cells respond to phytohormones to ultimately limit axial cell expansion.

Table 1. List of Arabidopsis (*Arabidopsis thaliana*) lines utilized in this study

Line name/ABRC no.	Abbreviation	References
Columbia -0	Col-0	
SALK_015615	*wdl4*	
axr2.1/CS3077	—	Wilson et al. 1990
35s:GFP-EB1b	GFP-EB1	Mathur et al. 2003
35s:GFP-Tub1	GFP-TUB1	Cutler & Ehrhardt, 2002
DR5:GFP	DR5:GFP	Ulmasov et al. 1997
axr2.1/35s:GFP-TUB1	*axr2.1*	True and Shaw 2020

Materials and methods

Plant lines

All Arabidopsis (*Arabidopsis thaliana*) lines were in the Columbia-0 background (Col-0) and are listed in Tables 1 and 2. Briefly, to create proWDL4:WDL4:mNeon, the *WDL4* genomic sequence, including 1.4 kb of upstream sequence (*proWDL4*:*WDL4*) was isolated from Col-0 genomic DNA. Using gateway cloning, proWDL4:WDL4 was fused to mNeon (sequence synthesized and codon optimized to be expressed in Arabidopsis) in the pEG301 vector backbone (Earley et al. 2006). Transgenic lines were created using the floral dip method (Bent 2006). T1 lines were isolated after BASTA (glufosinate ammonium; Cayman Chemical) selection and crossed into *wdl4* background. T3 lines were sequenced for homozygous tDNA insertion. At least 2 separate lines were used in all experiments. The WDL4 constitutively expressed line was created by cloning the genomic WDL4-mNeon DNA and inserting into the pEG100 backbone (Earley et al. 2006) to produce 2 × 35s:WDL4:mNeon before floral dipping into Col-0. T1 lines were isolated after BASTA selection, and at least 2 T3 lines were used for experiments.

The 2 × 35s:mScarlet:Tub1 was created using the genomic TUB1 (AT1G75780) coding sequence amplified from Col-0 genomic DNA using primers listed in Supplemental Table S1. The mScarlet fluorescent protein coding sequence was codon-optimized for Arabidopsis and synthesized by Genscript (Piscataway, NJ). 2 × 35s:mScarlet-TUB1 and a BASTA resistance gene were assembled into Golden Gate destination vector pAGM4673 (Weber et al. 2011) and sequence verified. The resulting construct was transformed into Col-0 plants using the *Agrobacterium*-mediated floral dip method (Bent 2006).

Plant growth conditions

Seeds were surface-sterilized (19:1 v/v solution of 87.5% ethanol and 30% hydrogen peroxide), dried, and sown on ½ Murashige and Skoog (MS) medium with a vitamin supplement and 1% agar (v/w). Seeds were stratified on plates in

Table 2. List of lines created specifically for this study. Vector backbones used to the transform germline are listed along reference when appropriate. Abbreviations listed are the ones used in the text

Created lines	Abbreviation	Vector backbone[a]	Vector reference	Means of creation
2 × 35s:WDL4-mNeon/Col-0	35s:WDL4	pEG100	Earley et al. 2006	Floral dip
proWDL4:WDL4-mNeon/Col-0		pEG301	Earley et al. 2006	Floral dip
proWDL4:WDL4-mNeon/SALK_015615	proWDL4:WDL4			Cross
SALK_015615/35s:GFP-TUB1	*wdl4*			Cross
SALK_015615/35s:GFP-EB1b	*wdl4*/*EB1*			Cross
SALK_015615/*axr2.1*/35s:GFP-TUB1	*wdl4*/axr2.1			Cross
2 × 35s:mScarlet-TUB1/Col-0	RFP-TUB1	pAGM4673	Engler et al. 2014	Floral dip
proWDL4:WDL4-mNeon/2 × 35s:mScarlet-TUB1/Col-0	proWDL4/RFP-TUB1			Cross

[a]Vector backbone used for floral dipping when applicable.

the dark at 4 °C for at least 48 h. For all experiments, seedlings were grown vertically and at 22 °C in constant light unless otherwise mentioned. For etiolated seedlings, seeds were exposed to white light for 7 h at 22 °C then covered and grown at 22 °C until mentioned time points. For de-etiolated seedlings, after stratification seedlings were grown at 22 °C in continuous white light or 12 h light/12 h dark cycle. For temperature shift experiments, seedlings were grown at 22 °C in continuous white light for 24 h before being shifted to 28 °C room with constant white light. For hormone and auxinole (10 µM) (Hayashi et al. 2012) treatment, seedlings were grown on nylon mesh (10 µm) on ½ MS plates for 3 d after stratification. The nylon mesh with seedlings was then transferred to the treatment plate for 3 d before hypocotyl measurement.

Phenotype analysis

Hypocotyl length measurements were taken from seedlings imaged on an Olympus stereo-microscope with a CCD camera using a millimeter ruler on the medium surface for reference. Measurements were made using FIJI (FIJI Is Just ImageJ) after converting pixels to micrometers. For all light grown experiments, the same seedlings were measured at each reported time point.

To image pWDL4:WDL4-NEON localization, seedlings were mounted in 1/2× MS and imaged using a Leica SP8 LSCM with 488 nm excitation, variably tuned emission window, a 40× 1.2 NA objective and utilizing the temporal gating to limit plastid autofluorescence. Images of whole seedlings Z-stacks of 1 µm were taken from the outermost surface of the hypocotyl through the epidermal layer. A 3D reconstruction of the entire hypocotyl was produced in FIJI for presentation. IMARIS 3D reconstruction was used to visualize WDL4-mNEON and microtubule localization on different cell faces.

For cell length measurements, 4 dpg seedlings were bathed in propidium iodide diluted in water (final concentration of 1 µg/µL w/v) for 2 min, washed, and imaged on the Nikon A1 LSCM using 561 nm excitation, 580 ± 20 nm emission filter, and a 20× 0.9 NA objective. Sequential image stacks were taken to halfway through the epidermal cells. A maximum projection image of the entire hypocotyl was reconstructed using FIJI for import into a MATLAB GUI (Vineyard et al. 2013) where cells were measured and length converted to micrometers.

To observe microtubule array patterns, 5 dpg seedlings expressing GFP-TUB1 were incubated in ½ MS liquid media with either DMSO or 5 µM picloram for 2 h to induce transverse microtubules. For the 35s:WDL4 background, WDL4-mNEON array patterns were used as a proxy for microtubules. The hypocotyl face was reconstructed from maximum projections of overlapping LSCM 3D projections and imported into a MATLAB GUI where cortical microtubule pattern was assigned by eye for each cell along a minimum of 2 complete hypocotyl cell files (Vineyard et al. 2013). Cortical microtubule array patterns were assigned as either longitudinal, oblique, transverse, or basket patterns.DR5:GFP expression (Ulmasov et al. 1997) was visualized using a 4× objective on a Nikon A1 LSCM excited at 488 nm using a broad-band emission filter. Sequential image stacks were taken through the entire hypocotyl. Per experiment, each slide contained a non-GFP expressing control (Col-0), DR5:GFP in the Col0 background, and DR5:GFP in the *wdl4* background. Maximum intensity projections were analyzed using FIJI. In brief, each hypocotyl was divided into sections of equal length and width. For each section, the mean fluorescence intensity was recorded as well as the average fluorescence intensity of each column of pixels spanning the section to create a histogram. If there was an asymmetric fluorescence distribution, the brighter region was oriented to be on the left side. Since boxes were often wider than the hypocotyl, data from histograms were aligned to coincide with the edge of the hypocotyl. The mean fluorescence outside of the hypocotyl was used to determine the electronic offset for subtraction.

Statistical analysis

For hypocotyl lengths, a 2-tailed t-test of pooled length measures was used to compare between the experimental data set and the age matched control. Differences were considered statically significant when $P < 0.05$. For comparison of microtubule array patterns, a nonparametric rank sum test was performed comparing percentage of transverse patterns (normalized per plant) for each plant line to the wild-type control.

Accession numbers

Sequence data from this article can be found in the GenBank/EMBL data libraries under accession numbers WDL4 (AT2G35880), EB1b (AT5G62500), TUB1 (AT1G75780), and AXR2 (IAA7, AT3G23050).

Acknowledgments

We thank Jim Powers and Andras Kun for assistance at the Indiana University Light Microscopy Imaging Center.

Author contributions

K.S. planned, executed, and analyzed experiments and drafted the manuscript. A.C.B. and T.H. performed research. T.C. created the 35s:mScarlet-TUB1 line. A.E. executed and analyzed the EB1 experiments. S.L.S. contributed to the experimental design, statistical analyses, and preparation of the manuscript.

Supplemental data

The following materials are available in the online version of this article.

Supplemental Figure S1. pWDL4:WDL4-mNeon rescues *wdl4* growth phenotype.

Supplemental Figure S2. pWDL4:WDL4-mNeon is expressed throughout the hypocotyl.

Supplemental Figure S3. Cortical array pattern distribution at 4 and 6 dpg for wild type and *wdl4* hypocotyls.

Supplemental Figure S4. Normalized growth response to exogenous hormone treatments.

Supplemental Figure S5. ACC induces epinastic cotyledons in the *wdl4* mutant.

Supplemental Figure S6. Auxinole suppresses hypocotyl elongation in the *wdl4* mutant.

Supplemental Figure S7. Transverse distribution of auxin-dependent DR5:GFP expression in *wdl4* hypocotyls.

Supplemental Table 1. List of primers used to isolate genomic DNA.

Funding

Funding for this work was provided by NSF-MCB1927504 to S.L.S.

Conflict of interest statement. None declared.

Data availability

All data generated and analyzed for this research article are included in all Figures and Supplementary Figures and Tables.

References

Bent A. *Arabidopsis thaliana* floral dip transformation method. In: **Wang K**, editor. Agrobacterium protocols. Totowa (NJ): Humana Press; 2006. p. 87–103.

Braidwood L, Breuer C, Sugimoto K. My body is a cage: mechanisms and modulation of plant cell growth. New Phytol. 2014:**201**(2): 388–402. https://doi.org/10.1111/nph.12473

Chapman EJ, Greenham K, Castillejo C, Sartor R, Bialy A, Sun T-P, Estelle M. Hypocotyl transcriptome reveals auxin regulation of growth-promoting genes through GA-dependent and -independent pathways. PLoS One. 2012:**7**(5):e36210. https://doi.org/10.1371/journal.pone.0036210

Collett CE, Harberd NP, Leyser O. Hormonal interactions in the control of Arabidopsis hypocotyl elongation. Plant Physiol. 2000:**124**(2): 553–562. https://doi.org/10.1104/pp.124.2.553

Cosgrove DJ. Growth of the plant cell wall. Nat Rev Mol Cell Biol. 2005:**6**(11):850–861. https://doi.org/10.1038/nrm1746

Cosgrove DJ. Building an extensible cell wall. Plant Physiol. 2022:**189**(3): 1246–1277. https://doi.org/10.1093/plphys/kiac184

Cui X, Wang S, Huang Y, Ding X, Wang Z, Zheng L, Bi Y, Ge F, Zhu L, Yuan M, et al. Arabidopsis SYP121 acts as a ROP2 effector in the regulation of root hair tip growth. Mol Plant. 2022:**15**(6): 1008–1023. https://doi.org/10.1016/j.molp.2022.04.008

Cutler SR, Ehrhardt DW. Polarized cytokinesis in vacuolate cells of *Arabidopsis*. Proc Natl Acad Sci. 2002:**99**(5): 2812–2817. http://dx.doi.org/10.1073/pnas.052712299

Deng J, Wang X, Liu Z, Mao T. The microtubule-associated protein WDL4 modulates auxin distribution to promote apical hook opening in Arabidopsis. Plant Cell. 2021:**33**(6):1927–1944. https://doi.org/10.1093/plcell/koab080

Earley KW, Haag JR, Pontes O, Opper K, Juehne T, Song K, Pikaard CS. Gateway-compatible vectors for plant functional genomics and proteomics. Plant J. 2006:**45**(4):616–629. https://doi.org/10.1111/j.1365-313X.2005.02617.x

Elbasiouny H, El-Ramady H, Elbehiry F, Rajput VD, Minkina T, Mandzhieva S. Plant nutrition under climate change and soil carbon sequestration. Sustainability. 2022:**14**(2):914. https://doi.org/10.3390/su14020914

Elliott A, Shaw SL. Microtubule array patterns have a common underlying architecture in hypocotyl cells. Plant Physiol. 2018:**176**(1): 307–325. https://doi.org/10.1104/pp.17.01112

Engler C, Youles M, Gruetzner R, Ehnert T-M, Werner S, Jones JDG, Patron NJ, Marillonnet S. A golden gate modular cloning toolbox for plants. ACS Synth Biol. 2014:**3**(11): 839–843. http://dx.doi.org/10.1021/sb4001504

Esmon CA, Pedmale UV, Liscum E. Plant tropisms: providing the power of movement to a sessile organism. Int J Dev Biol. 2005:**49**(5–6):665–674. https://doi.org/10.1387/ijdb.052028ce

Friml J. Fourteen stations of auxin. Cold Spring Harb Perspect Biol. 2022:**14**(5):a039859. https://doi.org/10.1101/cshperspect.a039859

Fujiwara M, Uemura T, Ebine K, Nishimori Y, Ueda T, Nakano A, Sato MH, Fukao Y. Interactomics of Qa-SNARE in *Arabidopsis thaliana*. Plant Cell Physiol. 2014:**55**(4):781–789. https://doi.org/10.1093/pcp/pcu038

Gendreau E, Traas J, Desnos T, Grandjean O, Caboche M, Höfte H. Cellular basis of hypocotyl growth in *Arabidopsis thaliana*. Plant Physiol. 1997:**114**(1):295–305. https://doi.org/10.1104/pp.114.1.295

Granger CL, Cyr RJ. Spatiotemporal relationships between growth and microtubule orientation as revealed in living root cells of *Arabidopsis thaliana* transformed with green-fluorescent-protein gene construct GFP-MBD. Protoplasma. 2001:**216**(3–4):201–214. https://doi.org/10.1007/BF02673872

Gray WM, Östin A, Sandberg G, Romano CP, & Estelle M. High temperature promotes auxin-mediated hypocotyl elongation in *Arabidopsis*. Proc Natl Acad Sci USA. 1998:**95**(12):7197–7202. https://doi.org/10.1073/pnas.95.12.7197

Hamaker JW, Johnston H, Martin RT, Redemann CT. A picolinic acid derivative: a plant growth regulator. Science. 1963:**141**(3578):363. https://doi.org/10.1126/science.141.3578.363

Hayashi K-I, Neve J, Hirose M, Kuboki A, Shimada Y, Kepinski S, Nozaki H. Rational design of an auxin antagonist of the SCFTIR1

auxin receptor complex. ACS Chem Biol. 2012:**7**(3):590–598. https://doi.org/10.1021/cb200404c

Li J, Nagpal P, Vitart V, Mcmorris TC, Chory J. A role for brassinosteroids in light-dependent development of Arabidopsis. Science. 1996:**272**(5260):398–401. https://doi.org/10.1126/science.272.5260.398

Lian N, Liu X, Wang X, Zhou Y, Li H, Li J, Mao T. COP1 Mediates dark-specific degradation of microtubule-associated protein WDL3 in regulating Arabidopsis hypocotyl elongation. Proc Natl Acad Sci USA. 2017:**114**(46):12321–12326. https://doi.org/10.1073/pnas.1708087114

Liang X, Wang H, Mao L, Hu Y, Dong T, Zhang Y, Wang X, Bi Y. Involvement of COP1 in ethylene- and light-regulated hypocotyl elongation. Planta. 2012:**236**(6):1791–1802. https://doi.org/10.1007/s00425-012-1730-y

Liu X, Qin T, Ma Q, Sun J, Liu Z, Yuan M, Mao T. Light-regulated hypocotyl elongation involves proteasome-dependent degradation of the microtubule regulatory protein WDL3 in Arabidopsis. Plant Cell. 2013:**25**(5):1740–1755. https://doi.org/10.1105/tpc.113.112789

Mathur J, Mathur N, Kernebeck B, Srinivas BP, Hülskamp M. A novel localization pattern for an EB1-like protein links microtubule dynamics to endomembrane organization. Curr Biol. 2003:**13**(22):1991–1997. https://doi.org/10.1016/j.cub.2003.10.033

Oda Y. Cortical microtubule rearrangements and cell wall patterning. Front Plant Sci. 2015:**6**:236. https://doi.org/10.3389/fpls.2015.00236

Oh E, Zhu J-Y, Bai M-Y, Arenhart RA, Sun Y, Wang Z-Y. Cell elongation is regulated through a central circuit of interacting transcription factors in the Arabidopsis hypocotyl. eLife. 2014:**3**:e03031. https://doi.org/10.7554/eLife.03031

Paredez AR, Somerville CR, Ehrhardt DW. Visualization of cellulose synthase demonstrates functional association with microtubules. Science. 2006:**312**(5779):1491–1495. https://doi.org/10.1126/science.1126551

Poór P, Nawaz K, Gupta R, Ashfaque F, Khan MIR. Ethylene involvement in the regulation of heat stress tolerance in plants. Plant Cell Rep. 2022:**41**(3):675–698. https://doi.org/10.1007/s00299-021-02675-8

Reed JW, Wu M-F, Reeves PH, Hodgens C, Yadav V, Hayes S, Pierik R. Three auxin response factors promote hypocotyl elongation. Plant Physiol. 2018:**178**(2):864–875. https://doi.org/10.1104/pp.18.00718

Reid R, Hayes J. Mechanisms and control of nutrient uptake in plants. Int Rev Cytol. 2003:**229**(2003):73–115. https://doi.org/10.1016/S0074-7696(03)29003-3

Sanderfoot AA, Kovaleva V, Bassham DC, Raikhel NV. Interactions between syntaxins identify at least five SNARE complexes within the Golgi/prevacuolar system of the Arabidopsis cell. Mol Biol Cell. 2001:**12**(12):3733–3743. https://doi.org/10.1091/mbc.12.12.3733

Sedbrook JC, Kaloriti D. Microtubules, MAPs and plant directional cell expansion. Trends Plant Sci. 2008:**13**(6):303–310. https://doi.org/10.1016/j.tplants.2008.04.002

Shaner NC, Lambert GG, Chammas A, Ni Y, Cranfill PJ, Baird MA, Sell BR, Allen JR, Day RN, Israelsson M, et al. A bright monomeric green fluorescent protein derived from Branchiostoma lanceolatum. Nat Methods. 2013:**10**(5):407–409. https://doi.org/10.1038/nmeth.2413

Shaw SL, Kamyar R, Ehrhardt DW. Sustained microtubule treadmilling in Arabidopsis cortical arrays. Science. 2003:**300**(5626):1715–1718. https://doi.org/10.1126/science.1083529

Shibaoka H. Plant hormone-induced changes in the orientation of cortical microtubules: alterations in the cross-linking between microtubules and the plasma membrane. Annu Rev Plant Biol. 1994:**45**(1):527–544. https://doi.org/10.1146/annurev.pp.45.060194.002523

Smalle J, Haegman M, Kurepa J, Van Montagu M, Straeten DV. Ethylene can stimulate Arabidopsis hypocotyl elongation in the light. Proc Natl Acad Sci U S A. 1997:**94**(6):2756–2761. https://doi.org/10.1073/pnas.94.6.2756

Smertenko A, Clare SJ, Effertz K, Parish A, Ross A, Schmidt S. A guide to plant TPX2-like and WAVE-DAMPENED2-like proteins. J Exp Bot. 2021:**72**(4):1034–1045. https://doi.org/10.1093/jxb/eraa513

Spartz AK, Lee SH, Wenger JP, Gonzalez N, Itoh H, Inzé D, Peer WA, Murphy AS, Overvoorde PJ, Gray WM. The SAUR19 subfamily of SMALL AUXIN UP RNA genes promote cell expansion. Plant J. 2012:**70**(6):978–990. https://doi.org/10.1111/j.1365-313X.2012.04946.x

Sun J, Ma Q, Mao T. Ethylene regulates the Arabidopsis microtubule-associated protein WAVE-DAMPENED2-LIKE5 in etiolated hypocotyl elongation. Plant Physiol. 2015:**169**(1):325–337. https://doi.org/10.1104/pp.15.00609

Takahashi K, Hayashi K, Kinoshita T. Auxin activates the plasma membrane H+-ATPase by phosphorylation during hypocotyl elongation in Arabidopsis. Plant Physiol. 2012:**159**(2):632–641. https://doi.org/10.1104/pp.112.196428

Thoms D, Vineyard L, Elliott A, Shaw SL. CLASP facilitates transitions between cortical microtubule array patterns. Plant Physiol. 2018:**178**(4): 1551–1567. http://dx.doi.org/10.1104/pp.18.00961

True JH, Shaw SL. Exogenous auxin induces transverse microtubule arrays through TRANSPORT INHIBITOR RESPONSE1/AUXIN SIGNALING F-BOX receptors. Plant Physiol. 2020:**182**(2):892–907. https://doi.org/10.1104/pp.19.00928

Uemura T, Kim H, Saito C, Ebine K, Ueda T, Schulze-Lefert P, Nakano A. Qa-SNAREs localized to the trans-Golgi network regulate multiple transport pathways and extracellular disease resistance in plants. Proc Natl Acad Sci USA. 2012:**109**(5):1784–1789. https://doi.org/10.1073/pnas.1115146109

Ulmasov T, Murfett J, Hagen G, Guilfoyle TJ. Aux/IAA proteins repress expression of reporter genes containing natural and highly active synthetic auxin response elements. Plant Cell. 1997:**9**(11):1963–1971. https://doi.org/10.1105/tpc.9.11.1963

Vandenbussche F, Petrášek J, Žádníková P, Hoyerová K, Pešek B, Raz V, Swarup R, Bennett M, Zažímalová E, Benková E, et al. The auxin influx carriers AUX1 and LAX3 are involved in auxin-ethylene interactions during apical hook development in Arabidopsis thaliana seedlings. Development. 2010:**137**(4):597–606. https://doi.org/10.1242/dev.040790

Vandenbussche F, Verbelen J-P, Van Der Straeten D. Of light and length: regulation of hypocotyl growth in Arabidopsis. BioEssays. 2005:**27**(3):275–284. https://doi.org/10.1002/bies.20199

Verma V, Ravindran P, Kumar PP. Plant hormone-mediated regulation of stress responses. BMC Plant Biol. 2016:**16**(1):86. https://doi.org/10.1186/s12870-016-0771-y

Vineyard L, Elliott A, Dhingra S, Lucas JR, Shaw SL. Progressive transverse microtubule array organization in hormone-induced Arabidopsis hypocotyl cells. Plant Cell. 2013:**25**(2):662–676. https://doi.org/10.1105/tpc.112.107326

Waghmare S, Lileikyte E, Karnik R, Goodman JK, Blatt MR, Jones AME. SNAREs SYP121 and SYP122 mediate the secretion of distinct cargo subsets. Plant Physiol. 2018:**178**(4):1679–1688. https://doi.org/10.1104/pp.18.00832

Weber E, Engler C, Gruetzner R, Werner S, Marillonnet S. A modular cloning system for standardized assembly of multigene constructs. PLoS One. 2011:**6**(2):e16765. https://doi.org/10.1371/journal.pone.0016765

Wilson AK, Pickett FB, Turner JC, Estelle M. A dominant mutation in Arabidopsis confers resistance to auxin, ethylene and abscisic acid. Mol Gen Genet. 1990:**222**(2–3):377–383. https://doi.org/10.1007/BF00633843

Yu Y, Wang J, Zhang Z, Quan R, Zhang H, Deng XW, Ma L, Huang R. Ethylene promotes hypocotyl growth and HY5 degradation by enhancing the movement of COP1 to the nucleus in the light. PLoS Genet. 2013:**9**(12):e1004025. https://doi.org/10.1371/journal.pgen.1004025